BBA - General Subjects 1863 (2019) 456–465

Contents lists available at ScienceDirect

BBA - General Subjects

journal homepage: www.elsevier.com/locate/bbagen

Sp140 is a multi-SUMO-1 target and its PHD finger promotes SUMOylation of the adjacent Bromodomain

Chiara Zucchelli[a,1], Simone Tamburri[b,c,1], Giuseppe Filosa[b,2], Michela Ghitti[a], Giacomo Quilici[a], Angela Bachi[b,*], Giovanna Musco[a,*]

[a] Biomolecular NMR Unit c/o IRCCS S. Raffaele, Via Olgettina 58, 20132 Milano, Italy
[b] IFOM-FIRC Institute of Molecular Oncology, Via Adamello 16, 20139 Milano, Italy
[c] San Raffaele Vita-Salute University, Via Olgettina 60, 20132 Milano, Italy

ARTICLE INFO

Keywords:
Sp140
PHD
Bromodomain
SUMOylation
Proteomics
NMR

ABSTRACT

Background: Human Sp140 protein is a leukocyte-specific member of the speckled protein (Sp) family (Sp100, Sp110, Sp140, Sp140L), a class of multi-domain nuclear proteins involved in intrinsic immunity and transcriptional regulation. Sp140 regulates macrophage transcriptional program and is implicated in several haematologic malignancies. Little is known about Sp140 structural domains and its post-translational modifications.
Methods: We used mass spectrometry and biochemical experiments to investigate endogenous Sp140 SUMOylation in Burkitt's Lymphoma cells and Sp140 SUMOylation sites in HEK293T cells, FLAG-Sp140 transfected and His_6-SUMO-1^{T95K} infected. NMR spectroscopy and *in vitro* SUMOylation reactions were applied to investigate the role of Sp140 PHD finger in the SUMOylation of the adjacent BRD.
Results: Endogenous Sp140 is a SUMO-1 target, whereby FLAG-Sp140 harbors at least 13 SUMOylation sites distributed along the protein sequence, including the BRD. NMR experiments prove direct binding of the SUMO E2 ligase Ubc9 and SUMO-1 to PHD-BRD_{Sp140}. *In vitro* SUMOylation reactions show that the PHD_{Sp140} behaves as SUMO E3 ligase, assisting intramolecular SUMOylation of the adjacent BRD.
Conclusions: Sp140 is multi-SUMOylated and its PHD finger works as versatile protein-protein interaction platform promoting intramolecular SUMOylation of the adjacent BRD. Thus, combinatorial association of Sp140 chromatin binding domains generates a multifaceted interaction scaffold, whose function goes beyond the canonical histone recognition.
General significance: The addition of Sp140 to the increasing lists of multi-SUMOylated proteins opens new perspectives for molecular studies on Sp140 transcriptional activity, where SUMOylation could represent a regulatory route and a docking surface for the recruitment and assembly of leukocyte-specific transcription regulators.

1. Introduction

Human Sp140 is a nuclear leukocyte-specific protein, preferentially expressed in mature B cells, plasma cell lines, macrophages and granulocytes [1]. It is a member of the speckled protein (Sp) family (Sp100, Sp110, Sp140 and Sp140L), a class of multi-domain nuclear proteins mainly involved in intrinsic immunity and transcriptional regulation. It localizes to sub-nuclear structures containing Sp100 but devoid of PML [2]. In line with its leukocyte specificity, Sp140 is implicated in several immunological disorders, working as autoantigen in the serum of Primary Biliary Cirrhosis patients [2,3] and contributing to the innate immune response to HIV-1 by its interaction with the viral Vif protein [4]. Moreover, genome wide association studies have linked the *SP140* locus to different autoimmune diseases, such as multiple sclerosis [5–7] and Crohn's disease [8,9]. Finally, increasing evidences support its involvement in haematologic malignancies, including chronic lymphocytic leukemia (CLL) and multiple myeloma (MM). Indeed, nucleotide polymorphisms in *SP140* gene have been correlated with lower mRNA expression and higher CLL incidence [10–13] and several truncations or missense-mutations within *SP140* in the mutational profiles of MM patients suggest a possible onco-suppressor activity for Sp140 [14]. Despite its involvement in numerous immuno-pathological conditions,

* Corresponding authors.
E-mail addresses: angela.bachi@ifom.eu (A. Bachi), musco.giovanna@hsr.it (G. Musco).
[1] These authors contributed equally to the work.
[2] Present Address: PD Biometrics Department, F. Hoffmann-La Roche Ltd. Hochstrasse 16, CH-4053 Basel, Switzerland.

https://doi.org/10.1016/j.bbagen.2018.11.011
Received 13 June 2018; Received in revised form 25 October 2018; Accepted 16 November 2018
Available online 19 November 2018

Sp140 function is highly elusive and its role in immune response in physiological and pathological conditions is just starting to be elucidated [1]. Recent ChIP-Seq analysis has shown that Sp140 plays an essential role in repressing lineage-inappropriate genes in macrophages [1] and that it participates in chromatin-mediated regulation of gene expression [2,15]. Sp140 involvement in transcriptional regulation is well in keeping with the presence of several chromatin related modules. Similarly to Sp100C, the longest Sp100 isoform [16], Sp140 harbors a nuclear localization signal (NLS), a domain Caspase activation and recruitment (CARD) domain, a Sp-100 –AIRE- NucP41/75- and DEAF1 (SAND) domain [17] and a plant homeodomain (PHD) finger domain immediately followed by a Bromodomain (BRD). Both PHD finger and BRD are evolutionary conserved domains present in human chromatin-associated proteins, typically working as reader/effector modules able to recognize different histone post-translational modifications (PTMs) [18–20]. These two domains are often found in close sequence proximity (with less than 30 amino-acids as linker) and can thus form a structural-functional unit with diversified activities [21]. The PHD-BRD cassette allows for the combinatorial recognition of multivalent histone PTMs such as lysine methylation and acetylation [22], as observed for PHD-BRD$_{TRIM24}$ [23,24] or PHD-BRD$_{TRIM33}$ [25]. PHD-BRD$_{Sp140}$ has been shown to bind to unmodified histone H3 tail *in vitro*, whereby the BRD$_{Sp140}$ binds to acetylated histones Lysines without any specificity towards particular histone Lysines, possibly because of the absence of a conserved Asparagine in the BRD histone binding pocket [20,26]. The PHD-BRD cassette can also work as structural platform to facilitate intramolecular SUMOylation, as reported for Kap1/TRIM28, where intramolecular SUMOylation of the BRD promotes Kap1/TRIM28 mediated transcriptional silencing [27]. SUMOylation consists in the covalent attachment of the ubiquitin-like SUMO (Small Ubiquitin-related MOdifier) protein to Lysines of a target substrate. It is a highly dynamic post-translational modification involved in a wide range of nuclear processes, such as gene expression, genome stability [28], DNA damage response [29], protein trafficking [30] and cell cycle control [28]. The phylogenetic proximity of PHD-BRD$_{Sp140}$ with PHD-BRD$_{Kap1/TRIM28}$ [20], along with the high sequence homology between Sp140 and Sp100 protein, a well-known target of nuclear SUMOylation [31], prompted us to ask whether Sp140, and in particular its BRD, could be SUMOylated. Here we report for the first time that endogenous Sp140 is a SUMO-1 target in Daudi (Burkitt's Lymphoma) cell line. Moreover, using a proteomic strategy we demonstrate that FLAG-Sp140 is multi-SUMOylated in HEK293T cells infected with His$_6$-SUMO-1^{T95K}, with at least 13 SUMOylation sites distributed along the protein sequence, including the BRD. Furthermore, NMR experiments, proving direct binding of the SUMO E2 ligase Ubc9 and SUMO-1 to PHD-BRD$_{Sp140}$, and *in vitro* SUMOylation reactions show that PHD-BRD$_{Sp140}$ is a SUMO-1 target and PHD$_{Sp140}$ works as versatile protein-protein interaction platform, assisting intramolecular SUMOylation of the adjacent BRD.

2. Materials and methods

Details on immunofluorescence, cell cultures, subcellular fractionation, cellular transfections, lentiviral infections, quantitative real time PCR analysis, plasmids, immunoblotting and antibodies, SUMOplot™ analysis, sample preparation for mass spectrometry analysis, purification of His$_6$-SUMO-1^{T95K} from infected HEK293T cells, peptides and proteins identification by database searching are described in Supporting Information.

2.1. Endogenous SUMO-1 immunoprecipitation

Daudi cells were fractionated as described in Supporting Information. For immunoprecipitation of endogenous SUMO-1, nuclear extracts (10 mg) were incubated with 10 μg of anti SUMO-1 antibody and then 40 μl slurry of Sepharose Protein G beads were added for 2 h at 4 °C. IgG were used as negative control. Beads were washed with NEB buffer (details in Supporting Information) and immunocomplexes were eluted in Laemmli buffer and resolved on NuPAGE 4–12% precast protein gels (Invitrogen).

2.2. Identification of SUMOylated di-Gly peptides in HEK293 cells infected with His$_6$-SUMO-1^{T95K} and transfected with pFLAG-SP140-CMV-5a

After protease digestion by Lys-C, di-Gly peptides were enriched by immunoaffinity purification using the PTMScan® Ubiquitin Remnant Motif (K-ε-GG) Kit protocol (Cell Signaling). Briefly, digested peptides were purified by Sep-Pak®C18 (WAT051910, Waters Corporation), lyophilized for two days, re-suspended in appropriate IAP buffer (PTMScan® Ubiquitin Remnant Motif (K-ε-GG) Kit) and immunoprecipitated using anti di-Gly antibody coupled to beads for 2 h at 4 °C on the wheel. Then, beads were centrifuged at 2000*g* for 30 s and washed twice with Milli-Q water. Enriched peptides were then eluted from beads using 0.15% TFA at room temperature for 10 min. Eluted peptides were concentrated by vacuum concentrator and further purified by using C18 StageTip, as described above. Approximately 5 μl of purified peptide mixture were subjected to RP-HPLC on-line coupled with ESI-MS/MS. The same procedure was adopted for the double digested sample.

Purified peptides were analyzed as technical duplicate on a LC–ESI–MS-MS quadrupole Orbitrap Q-Exactive mass spectrometer (Thermo Fisher Scientific). Peptides were separated on a linear gradient from 95% solvent A (2% ACN, 0.1% formic acid) to 30% solvent B (80% acetonitrile, 0.1% formic acid) over 90 min and from 30 to 95% solvent B in 10 min at a constant 0.25 μl/min flow rate on UHPLC Easy-nLC 1000 (Thermo Scientific) connected to a 25-cm fused-silica emitter of 75 μm inner diameter (New Objective, Inc. Woburn, MA, USA), packed in-house with ReproSil-Pur C18-AQ 1.9 μm beads (Dr Maisch Gmbh, Ammerbuch, Germany) using a high-pressure bomb loader (Proxeon,Odense,Denmark).

MS data were acquired using a data-dependent (DDA) top 12 method for HCD fragmentation. Survey full scan MS spectra (300–1800 Th) were acquired in the Orbitrap Q-Exactive with 70,000 resolution, AGC target 3^{e6}, IT 10 ms. For HCD spectra, resolution was set to 35,000 at m/z 200, AGC target 5^{e4}, IT 120 ms; NCE 25% and isolation width 2.5 m/z.

2.3. Expression and purification of recombinant proteins

pETM11 expression vector (EMBL) was used for bacterial expression in BL21(DE3) *E. coli* cells of human PHD$_{Sp140}$ finger (residues M660-S711, NCBI accession code NP_001265380) and PHD-BRD$_{Sp140}$ (residues M660-N840; NCBI accession code NP_001265380). PHD$_{Sp140}$ was expressed and purified as described in [32]. PHD-BRD$_{Sp140}$ was similarly expressed and purified [32], using HiLoad 16/60 Superdex 75 pg column (GE Healthcare) for size exclusion chromatography and home-made His$_6$-TEV protease for cleavage of the His$_6$ tag. Both TEV and tag were subsequently removed by purification on Ni-NTA column. The final buffer contained 20 mM Na_2HPO_4/NaH_2PO_4 pH 6.3, 50 mM NaCl, 10 mM DTT and 50 μM $ZnCl_2$. His$_6$-GST tagged PHD-BRD$_{Sp140}$ (SP140PB) and His$_6$-GST-PHD$_{Sp140}$ (SP140PHD) were expressed in BL21(DE3) cells using pETM30 vector (EMBL) and purified like PHD-BRD$_{Sp140}$ but without tag cleavage. The double mutation K769R-K808R of SP140PB (SP140PB-K769R-K808R) was generated in the pETM30 vector by Genewiz and the mutant protein was expressed and purified as described for the wild type protein. Proteins identity was confirmed by mass spectroscopy. For NMR titration studies, uniformly ^{15}N-labelled PHD$_{Sp140}$ and PHD-BRD$_{Sp140}$ were expressed in *E. coli* BL21(DE3) cells in minimal media containing $^{15}NH_4Cl$ as sole nitrogen source, the His$_6$-tag was cleaved with TEV protease.

Mouse Ubc9 coding sequence was cloned from pET23a vector (kind gift by Dr. F. Melchior, DKFZ-ZMBH Alliance, Heidelberg, Germany) into the *NcoI/KpnI* sites of pETM11 vector (EMBL), after removal of an

internal NcoI site through PCR-site direct mutagenesis and conserving the coding sequence. Protein expression was obtained by BL21(DE3) *E. coli* induction for 4 h at 30 °C with 0.2 mM IPTG. Ubc9 was purified similarly to PHD-BRD$_{Sp140}$, with a final NMR buffer containing 20 mM Na_2HPO_4/NaH_2PO_4 pH 6.3, 150 mM NaCl, 5 mM DTT. Protein identity was confirmed by mass spectroscopy. Uniformly ^{15}N- and $^{15}N/^{13}C$-labelled Ubc9 was expressed in *E. coli* BL21(DE3) cells in minimal media containing $^{15}NH_4Cl$ and ^{13}C-glucose as sole nitrogen and carbon source.

The plasmid encoding wild type His$_6$-SUMO-1 was obtained by cloning SUMO-1 cDNA from pGEX-SUMO-1 vector (kind gift by Dr. R, Hay, Wellcome Trust Centre for Gene Regulation and Expression, Dundee, UK) into a pET-28a vector. His$_6$-SUMO-1 was purified like PHD-BRD$_{Sp140}$ without cleavage of the His$_6$-tag. The final NMR buffer contained 20 mM Na_2HPO_4/NaH_2PO_4 pH 6.8, 100 mM NaCl, 1 mM DTT. His$_6$-SUMO-1^{T95R} mutant was obtained by standard overlap extension method and purified from infected HEK293T cells as described in Supporting Information.

The plasmids encoding His$_6$-Aos1 subunit and Uba2 subunit (kindly provided by Dr. F. Melchior, DKFZ-ZMBH Alliance, Heidelberg, Germany) were cloned into pET-28a and pET-11d vectors, respectively. Purification of Aos1-Uba2 complex (SUMO E1 enzyme) was performed as described in [33].

2.4. In vitro SUMOylation reactions

In vitro SUMOylation reactions of His$_6$-GST-PHD-BRD$_{Sp140}$ (SP140PB) immobilized on Glutathione-Sepharose (GS) beads were performed at 30 °C, for 2 h under shaking, in a 40 µl reaction mix containing: 1.2 µg His$_6$-SUMO-1, 3 µg SP140PB, 1.4 µg Ubc9, 0.2 µg Aos1-Uba2 (E1 enzyme), 5 mM ATP, 5 mM NaCl, 20 mM HEPES pH 7.5, 5 mM $MgCl_2$, 0.05% Tween 20. Reactions without SP140PB, Ubc9 or E1 enzyme were used as controls. Reactions were stopped with 10 µl of reducing sample buffer and the samples were first boiled for 5 min at 95 °C and then loaded on Bolt 4–12% Bis-Tris Plus Gels precast protein gels (Invitrogen). Western blot was performed using Hybond™-ECL™ Amersham Biosciences nitrocellulose membrane, Tris-Glycine Transfer Buffer (25 mM Trizma base, 192 mM Glycine, 20% methanol, 0.1% SDS), TBS-T buffer (20 mM Tris-HCl, 0.5 M NaCl, 0.005% Tween 20), anti GST-HRP-conjugated antibody (Santa Cruz Biotechnology, dilution 1:2000) and ECL-Plus™ Western Blotting Reagents (Amersham Biosciences).

For cation chelation, SP140PB was immobilized on GS beads and extensively washed to eliminate $ZnCl_2$ from the buffer. Then, the protein was incubated with 100 µM of TPEN (N,N,N′,N′-tetrakis (2-pyridinylmethyl)-1,2-ethanediamine) or DMSO in reaction buffer, for 120 min at 30 °C. After extensive washings, the immobilized protein was used for *in vitro* SUMOylation, as described before. Control reactions with 3 µg of human GST-tagged RanGAP1 fragment (GST-RanGAP1, residues 418–587, Enzo Life Sciences), His$_6$-GST-PHD$_{Sp140}$ (SP140PHD) and SP140PB-K769R-K808R were performed as described for Sp140PB.

2.5. NMR spectroscopy

NMR experiments were performed at 298 K on a Bruker Avance 600 MHz spectrometer equipped with inverse triple resonance cryoprobe (TCI) and pulsed field gradients. Data were processed with Topspin 3.2 (Bruker) and analyzed with CcpNmr Analysis 2.1.5 [33]. Binding experiments were performed acquiring at each titration point a 2D water-flip-back ^{15}N-edited HSQC spectrum with 512 (100) complex points, 55 ms (60 ms) acquisition times, apodized by 60° shifted sine-bell squared (qsine) window function and zero filled to 1024 (512) points for ^1H (^{15}N), respectively. For ^{15}N PHD-BRD$_{Sp140}$, ^1H-^{15}N Trosy-HSQC experiments (bruker pulseprogram trosyf3gpphsi19.2) were acquired at 308 K, with 2048 (180) complex points, 100 ms (46 ms) acquisition times, apodized by 60° shifted sine-bell squared (qsine) window function and zero filled to 2048 (1024) points for ^1H (^{15}N), respectively. To investigate the effect of TPEN on PHD$_{Sp140}$ and PHD-BRD$_{Sp140}$ fold, we first removed $ZnCl_2$ in the protein buffer by dialysis, we incubated at room temperature for 3 h the sample with a 3-fold excess of TPEN and then we acquired ^1H-^{15}N HSQC (PHD$_{Sp140}$) and ^1H-^{15}N Trosy-HSQC (PHD-BRD$_{Sp140}$) experiments. Amides backbone assignment for free Ubc9 was obtained from CBCA(CO)NH and HNCA experiments [34,35] acquired on ^{15}N-^{13}C Ubc9 (1.34 mM, in 20 mM Na_2HPO_4/NaH_2PO_4 pH 6.3, 150 mM NaCl, 5 mM DTT). Amides backbone assignment for free PHD$_{Sp140}$ has been previously obtained [32]. Assignment of the resonances during all titrations series was made by following individual cross-peaks. For titration of ^{15}N PHD$_{Sp140}$ (0.2 mM) and ^{15}N PHD-BRD$_{Sp140}$, (0.38 mM) stock solutions of Ubc9 (6.7 mM) or His$_6$-SUMO-1 (3.7 mM) were stepwise added reaching the following molar ratios: ^{15}N PHD$_{Sp140}$:SUMO-1 1:2, ^{15}N PHD$_{Sp140}$:Ubc9 1:3, ^{15}N PHD-BRD$_{Sp140}$: Ubc9 and ^{15}N PHD-BRD$_{Sp140}$:His$_6$-SUMO-1 1:1.5. For titration of ^{15}N Ubc9 (0.1 mM), PHD$_{Sp140}$ (1.3 mM) or PHD-BRD$_{Sp140}$ (1.6 mM) were stepwise added up to a 4 fold excess. The weighted average of the ^1H and ^{15}N chemical shifts perturbation (CSP) upon binding was calculated as $CSP = [(\Delta^2 HN + \Delta^2 N/25)/2]^{1/2}$ [36]. Residues considered with significant CSP were those with normalized CSP > AVG + σ_{corr}, with σ_{corr} as defined in [37]. Protein concentrations were determined by UV spectroscopy using the following extinction coefficients at 280 nm: 5500 $M^{-1} cm^{-1}$, 22,920 $M^{-1} cm^{-1}$, 29,450 $M^{-1} cm^{-1}$ and 4470 $M^{-1} cm^{-1}$ for PHD$_{Sp140}$, PHD-BRD$_{Sp140}$, Ubc9 and His$_6$-SUMO-1, respectively.

2.6. Circular dichroism spectroscopy

CD spectra were acquired at 20 °C on a Jasco J-815 spectropolarimeter, equipped with a thermostatically controlled cell holder stabilized by circulating 20% ethanol. A rectangular quartz cuvette with 1 mm pathlength was used (Hellma). Each spectrum was averaged using four accumulations collected in 0.1 nm intervals with an average time of 0.5 s. Samples concentrations were 5 µM PHD-BRD$_{Sp140}$ and 20 µM PHD$_{Sp140}$ in 150 mM NaF, 20 mM NaH_2PO_4/Na_2HPO_4 pH 6.3. The observed ellipticity (mdeg) was converted into molar residue ellipticity [θ] (deg cm^2 $dmol^{-1}$). To monitor the effect of cation chelation on protein secondary structure, spectra were acquired after overnight incubation of the samples with 3-fold excess of TPEN.

2.7. Loops modelling of PHD-BRD$_{Sp140}$

We used the crystallographic structure of PHD-BRD$_{Sp140}$ in complex with short-chain variable fragment (Fv) (PDB ID: 6G8R) to map the PHD finger interaction with SUMO-1 and Ubc9 and to highlight the SUMOylation sites identified within the BRD. As the coordinates of the BC and the ZA loops and the one connecting the PHD and the BRD were not present in the pdb file, they were modelled with SWISSMODEL [38].

3. Results and discussion

3.1. Endogenous Sp140 is SUMOylated in Daudi cells

Inspired by the sequence homology between Sp140 and the SUMOylated proteins Sp100 [16,31] and Sp110 [39] (Supporting Information Fig. S1a) and prompted by SUMOPlot™ bioinformatics analysis predicting several putative SUMOylation sites within Sp140 sequence (Supporting Information Fig. S1b), we investigated whether also Sp140 was a SUMOylation substrate. We tested different cell lines for *SP140* expression and we chose Daudi cells as model system to study endogenous Sp140, as they showed the highest *SP140* mRNA levels (Supporting Information Fig. S2a) and Sp140 protein expression in the nucleus (Supporting Information Fig. S2b). To demonstrate that endogenous Sp140 is modified by SUMO-1, Daudi nuclear extract lysate

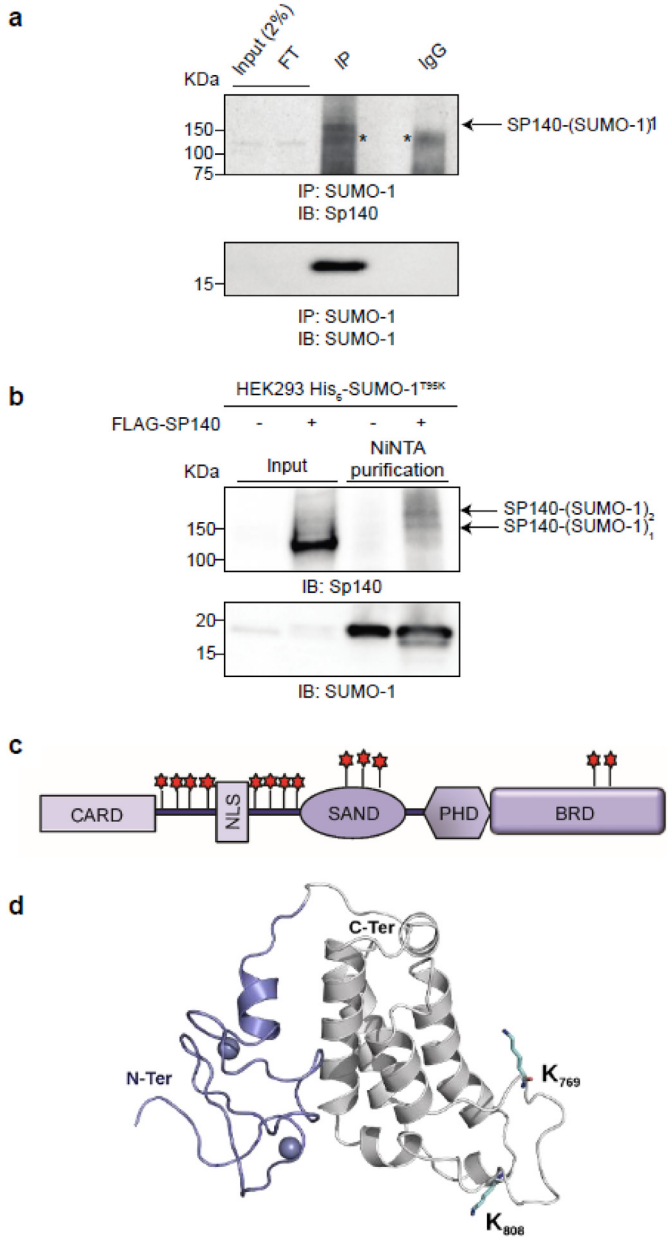

Fig. 1. Sp140 nuclear protein is SUMOylated.
(a) Immunoprecipitation of endogenous SUMO-1 in Daudi cells was performed with SUMO-1 antibody. Unrelated antibody (IgG) was used as negative control. The immuno-precipitated lysate was probed with anti-Sp140 antibody (upper panel) and with an anti-SUMO-1 antibody (bottom panel). The asterisk (*) indicates Heavy Chain (HC). The arrow indicates Sp140 SUMOylated fraction. Total lysate (Input), flow-through (FT), immunoprecipitation (IP). (b) Nickel Nitrilotriacetic acid affinity (NiNTA) purification was performed on HEK293T cells infected with His_6-SUMO-1^{T95K}, transfected or not (control) with FLAG-Sp140 vector and probed against Sp140. The arrows indicate Sp140 SUMOylated fractions. Total lysate (Input), Affinity enrichment of His SUMOylated proteins (NiNTA). (c) Sp140 domain architecture: CARD (Caspase activation and recruitment domain), SAND (Sp100, AIRE-1, NucP41/45, and DEAF-1 domain), PHD finger (plant homeodomain), BRD (Bromodomain) domains. Red stars indicate Lys-C-cleaved SUMOylation sites as determined by MS in cells. (d) Cartoon representation of PHD-BRD_{Sp140} structure (PDB ID: 6G8R) highlighting in blue and grey the PHD and BRD domains, respectively. Zn^{2+} ions are represented in spheres. K769 and K808 SUMOylation sites, located respectively on the so-called ZA and BC loops, are represented in cyan sticks.

was immunoprecipitated using an anti-SUMO-1 antibody and rabbit IgG as a control. Endogenous SUMO-1 immunoprecipitation, followed by immunoblot analysis with an antibody against Sp140, revealed a slower migrating, higher molecular weight band corresponding to the SUMOylated Sp140 protein (Fig. 1a, lane IP) that was absent in the control lane (lane IgG).

3.2. Mass spectrometry analysis enables identification of Sp140 SUMOylation sites

To date, the mass spectrometric identification of endogenous SUMOylation sites within a substrate is hampered by the large SUMO-1 branched peptide produced upon tryptic digestion. Therefore, to unambiguously identify SUMOylated peptides, we adopted a two-step strategy previously applied for SUMO-2 detection [40]. Briefly, SUMO-1 Threonine 95 was mutagenized into Lysine (SUMO-1^{T95K}) to introduce a Lys-C cleavage site upon enzymatic digestion producing a shorter GlyGly (di-Gly) SUMO-1 signature peptide containing the acceptor Lysine of the target protein (Supporting Information Fig. S3a). This strategy has also the advantage to avoid the identification of di-Gly containing peptides derived from ubiquitination that can be produced only by trypsin or Arg-C digestion. The di-Gly containing peptides are then enriched with an anti-Lys-di-Gly (KεGG) antibody and sequenced by mass spectrometry (MS) (Supporting Information Fig. S3b). As lentiviral infection of His_6-SUMO-1^{T95K} in Daudi had a very low efficiency, we selected HEK293T cells, which do not express endogenous *SP140* (Supporting Information Fig. S2a), as model system to investigate Sp140 SUMOylated sites. We transfected HEK293T cells with FLAG-Sp140 vector and we verified that the overexpressed protein behaves like the endogenous one, localizing to nuclear dots not overlapping with PML nuclear bodies, as observed for endogenous Sp140 in Daudi cells (Supporting Information Fig. S4a,b). Next, HEK293T cells were infected for the stable expression of His_6-SUMO-1^{T95K} and then transfected to overexpress FLAG-Sp140 (Supporting Information Fig. S4c). Enrichment of His_6-SUMO-1^{T95K} modified proteins through NiNTA affinity purification revealed the presence of two slower migrating bands corresponding to the SUMOylated fractions of Sp140 (Fig. 1b), confirming the results on endogenous Sp140 in Daudi cells (Fig. 1a). To precisely identify the SUMOylation sites within Sp140 sequence, we performed Lys-C digestion, followed by immunoprecipitation of di-Gly peptides and subsequent LC-MS/MS analysis (Supporting Information Fig. S3b). Herewith, we identified 13 SUMOylation sites in the full-length protein (Table 1, third column), whereby 6 were in agreement with the SUMOplot™ prediction.

The highest scored SUMO site predicted by SUMOplot™ (K735) was not identified by Lys-C digestion, but it was found in an independent experiment performed using Trypsin digestion (Table 1, the fourth column). This might be due to the length of the di-Gly peptide generated by Lys-C digestion, which prevents its identification by MS. In conclusion, the SUMOylation sites identified by MS span along the entire Sp140 sequence, mapping around the NLS, within the SAND domain and, most interestingly, within the BRD (K769, K808) (Table 1, Fig. 1c). K769 and K808 are in optimal position for post-translational modifications, as they are highly accessible and located on the flexible ZA (K769) and BC (K808) BRD loops (Fig. 1d), the latter in a position reminiscent of one of the sites identified in PHD-$BRD_{Kap1/Trim28}$ [27].

3.3. PHD-BRD_{Sp140} is SUMOylated in vitro

The identification of two SUMOylation sites within the BRD supports the notion that this domain constitutes a suitable target for SUMO-1 conjugation. Therefore, as a step forward in the molecular understanding of Sp140 as SUMOylation substrate, we focused our attention on its PHD-BRD cassette and asked whether the isolated tandem domain, similarly to PHD-$BRD_{Kap1/Trim28}$ [27] could be SUMOylated. We thus performed *in vitro* SUMOylation reactions using equal amounts

Table 1
Sp140 is SUMOylated at multiple sites. Identification of SUMOylation remnant peptides within FLAG-Sp140 protein expressed in HEK293T cells infected with His_6-SUMO-1^{T95K}. Some identified SUMOylation sites overlap with those predicted by SUMOplot™, whereas others are non-canonical (np = not predicted). For each identified GlyGly (di-Gly) peptide are reported: Gly-Gly positioning probabilities on Lysine (indicated in brackets), GlyGly (di-Gly) peptide position within Sp140 sequence, Posterior Error Probability (PEP) of the identified peptides after Lys-C digestion, Posterior Error Probability (PEP) of the identified peptides after Lys-C + Trypsin digestion and SUMOplot™ score.

GlyGly (K) probabilities	GlyGly (K) position	PEP Lys-C	PEP Lys-C + Trypsin	SUMOPlot score
LLPYGK(1)QENSNACHEMDDIAVPQEALSSSPR	162	–	0.000336325	0.67
CEPGFSSESCEQLALPK(1)AGGGDAEDAPSLLPGGGVSCK	204	–	4.58E-61	0.43
AGGGDAEDAPSLLPGGGVSCK(1)LAIQIDEGESEEMPK	225	5.56E-08	3.80E-27	np
LAIQIDEGESEEMPK(1)LLPYDTEVLESNGMIDAAR	240	–	4.17E-38	np
EK(1)YQESPEGRDKETFDLK	287	0.00000659	1.27E-07	np
YQESPEGRDK(1)ETFDLK	297	0.00000257	6.21E-69	np
ETFDLK(1)TPQVTNEGEPEK	303	2.74E-26	3.98E-75	0.8
CGSVSCLSAETFDLK(1)TPQVTNEGEPEK	303	–	2.85E-15	0.8
TESDQACGTMDTVDIANNSTLGK(0.982)PK(0.018)	467	–	2.10E-08	np
TESDQACGTMDTVDIANNSTLGK(0.166)PK(0.834)R	469	–	0.000604775	np
ADGQVVSSEK(0.974)K(0.026)	508	0.000351	4.08E-06	np
K(1)ANVNLK	509	0.000305	3.69E-15	np
ANVNLK(1)DLSK	515	0.000367	5.97E-06	np
RGK(1)PGTRFTQSDRAAQK	527	0.008314	–	0.5
K(0.998)HK(0.002)DETVDFK	550		2.64E-74	np
HK(1)DETVDFK	552	0.044537	5.82E-49	0.52
HKDETVDFK(1)APLLPVTCGGVK	559	0.013456	1.92E-05	0.74
APLLPVTCGGVK(0.998)GILHK(0.002)	571	–	0.000863385	np
K(1)LQQGILVK	578	–	0.000138752	np
CIQTEDGK(1)WFTPTEFEIK	594	0.015629	1.73E-37	0.32
RILK(1)SQNNSSVDPCMR	649	–	0.00952374	np
MK(1)ESPGSQQCCQESEVLER	709	–	0.0303255	np
QMCPEEQLK(1)CEFLLLK	735	–	1.72E-20	0.91
IPYYYYIREACQGLK(1)EPMWLDK	769	1.45E-10	0.000973155	0.8
RLNEHGYPQVEGFVQDMRLIFQNHRASYK(0.929)YK(0.071)	808	3.57E-11	–	np
YK(1)DFGQMGFR	810	–	6.89E-13	np

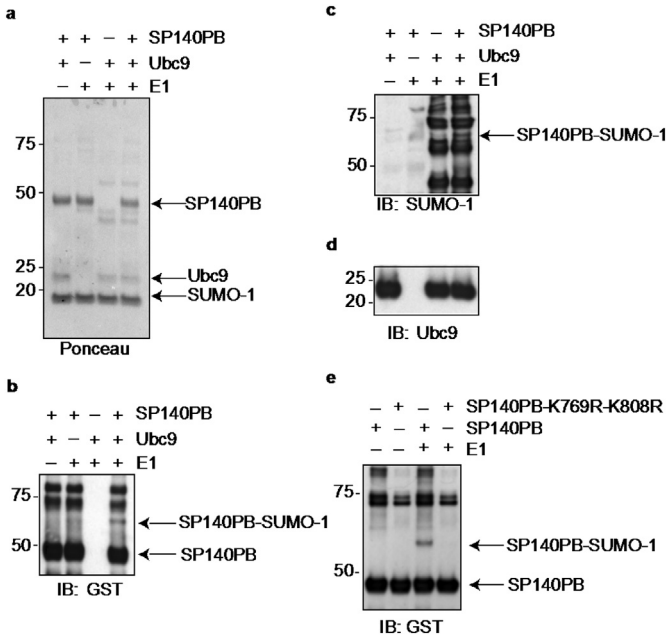

Fig. 2. PHD-BRD_{Sp140} is SUMOylated *in vitro*.
In vitro SUMOylation reaction of immobilized His_6-GST-PHD-BRD_{Sp140} (SP140PB) incubated for 120 min at 30 °C with His_6-SUMO-1 (2-fold excess), as shown by (a) Ponceau staining, (b) anti-GST, (c) anti-SUMO-1 and (d) anti-Ubc9 immunoblot analysis. Bands corresponding to the unmodified and SUMOylated protein are indicated with arrows. Reactions without E1 or E2 (Ubc9) enzymes were used as controls. (e) *In vitro* SUMOylation of immobilized SP140PB wild type and K769R-K808R mutant (SP140PB-K769R-K808R).

of recombinant His_6-GST-PHD-BRD_{Sp140} (SP140PB) and His_6-SUMO-1 plus all the components of the SUMOylation pathway (Fig. 2a–d).

Herein, amongst several bands corresponding to multimeric forms of SP140PB (likely due to the high protein concentration in the reaction) present in all lanes and to intermediates of the SUMOylation reaction, we observed a slow migrating band (~66 kDa), decorated by both anti GST (Fig. 2b) and anti SUMO antibodies (Fig. 2c), consistent with the conjugation to SP140PB (~48 kDa) of one His_6-SUMO-1 moiety (~18 kDa), whose formation was time dependent (Supporting Information Fig. S5a,b). Negative control reactions without the SUMOylation enzymes E1 or E2 (Ubc9) did not show any SUMOylation product. Importantly, *in vitro* SUMOylation reaction on the isolated His-GST tagged PHD finger of Sp140 (SP140PHD) did not present any evidence of SUMO-1 conjugation, in agreement with SUMOplot™ predictions and MS data (Fig. S5c, Table 1), thus supporting the notion that the PHD domain of Sp140 is not a substrate of SUMO-1. Conversely, mutations into Arginine of both K769 and K808 SUMOylation sites (SP140PB-K769R-K808R), located on the flexible ZA and BC BRD loops, abrogated SUMO-1 conjugation (Fig. 2e). Taken together, MS data and reconstituted SUMOylation reactions clearly show that the BRD within the context of full length Sp140 and of the isolated PHD-BRD_{Sp140} tandem domain is a suitable SUMOylation target both in cells and *in vitro*.

3.4. PHD-BRD_{Sp140} and PHD_{Sp140} interact with Ubc9 and SUMO-1

Next, we used NMR to assess PHD-BRD_{Sp140} direct interaction with the fundamental components of the SUMOylation reaction (Ubc9 and SUMO-1). To this aim we produced ^{15}N labelled PHD-BRD_{Sp140}. The good peaks dispersion of the ^{1}H-^{15}N Trosy-HSQC spectrum indicated that the domain was folded. Superposition of the 2D ^{1}H-^{15}N-HSQC spectra of PHD-BRD_{Sp140} and PHD_{Sp140} alone showed that the PHD_{Sp140} finger was strongly influenced by the BRD_{Sp140} presence, as only few peaks of the PHD_{Sp140} alone matched with those of the tandem domain (Supporting Information Fig. S6a,b). This observation is in agreement with the presence of extensive hydrophobic interactions between PHD_{Sp140} and the adjacent BRD_{Sp140}, which together form an integrated structure (Supporting Information Fig. S6c). At variance to PHD_{Sp140},

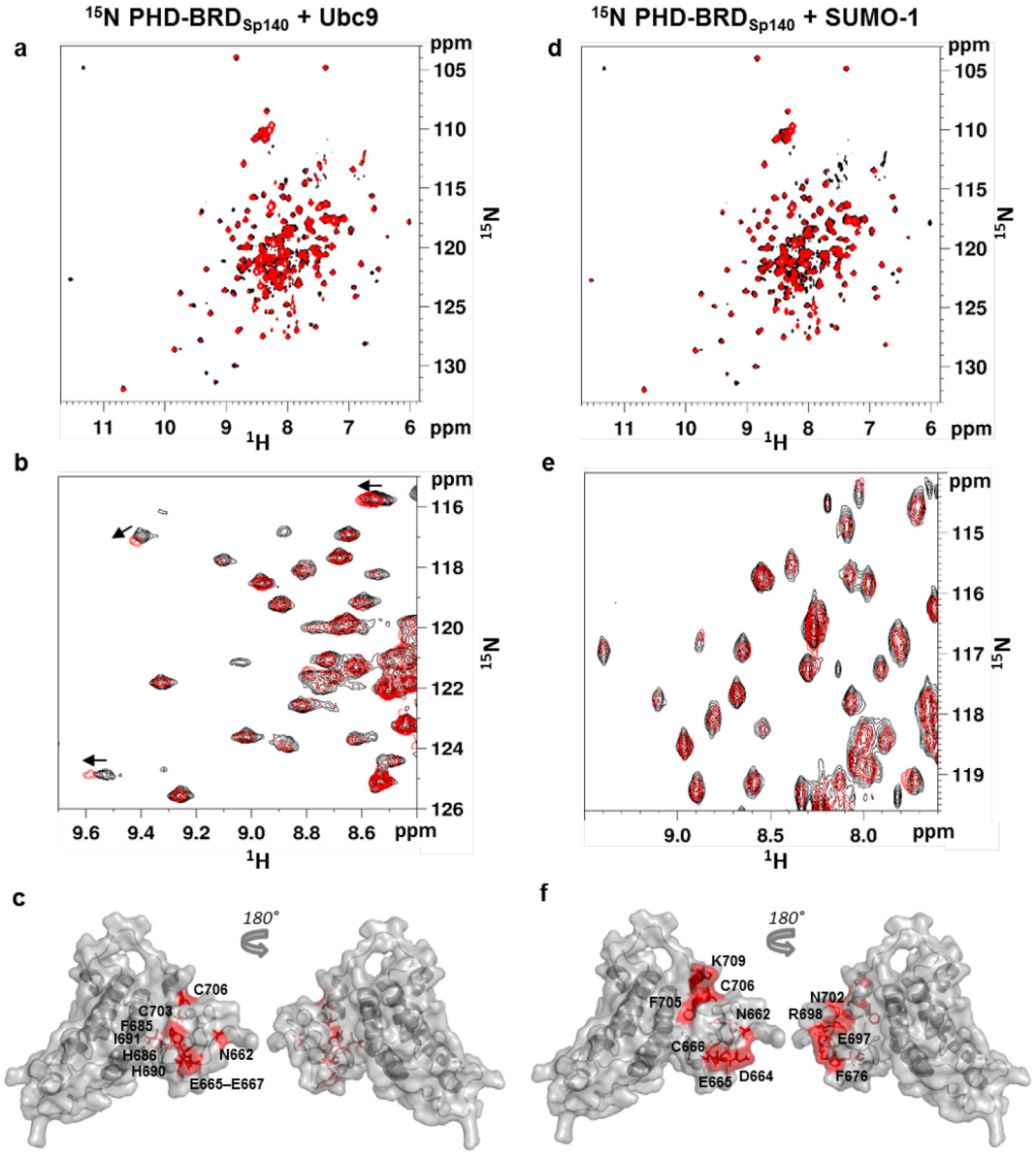

Fig. 3. ^{15}N PHD-BRD$_{Sp140}$ interacts with Ubc9 and SUMO-1.
(a) Superposition of the ^{1}H-^{15}N Trosy-HSQC spectra of 0.38 mM ^{15}N PHD-BRD$_{Sp140}$ without (black) and with (red) 1.5-fold excess of Ubc9. (b) A zoomed region of the overlaid spectra showing peaks shifting or disappearing. (c) Surface and cartoon representation of PHD-BRD$_{Sp140}$, PHD$_{Sp140}$ residues with CSP > AVG + σ_{corr} upon Ubc9 addition are labelled and highlighted in red (d) Superposition of the ^{1}H-^{15}N Trosy-HSQC spectra of 0.38 mM ^{15}N PHD-BRD$_{Sp140}$ without (black) and with (red) 1.5-fold excess of SUMO-1. (e) Zoomed region of the overlaid spectra showing peaks shifting or disappearing. (f). Surface and cartoon representation of PHD-BRD$_{Sp140}$, PHD$_{Sp140}$ residues with CSP > AVG + σ_{corr} upon SUMO-1 addition are labelled and highlighted in red.

the isolated BRD$_{Sp140}$ (both in His-tagged and GST form) was not soluble, supporting a role for PHD$_{Sp140}$ in shielding BRD$_{Sp140}$ exposed hydrophobic residues. However, several peaks in the ^{1}H-^{15}N Trosy-HSQC of PHD-BRD$_{Sp140}$ suffered of line-broadening effects, most likely deriving from conformational exchange phenomena (Supporting Information Fig. S6d). Accordingly, enhanced carbon R2 relaxation rates of several resonances in triple resonance experiments hampered backbone assignment of the tandem domain. Nevertheless, the spectra were sufficiently well resolved to observe a substantial number of PHD-BRD$_{Sp140}$ backbone amide resonances in the ^{1}H-^{15}N Trosy-HSQC spectrum shifting or disappearing upon Ubc9 addition (Fig. 3a,b). These effects, in strong analogy to BRD-PHD$_{Kap1/TRIM28}$ [27], suggested the presence of slow-intermediate exchange phenomena in the NMR time scale, indicative of low micro-molar binding affinity. Similarly to PHD$_{Kap1/TRIM28}$ [41], the isolated PHD$_{Sp140}$ was also able to weakly interact with Ubc9, as proved by small but significant chemical shift perturbations (CSPs) upon addition of Ubc9 to ^{15}N PHD$_{Sp140}$ (Supporting Information Fig. S7a,b).

When mapped on PHD-BRD$_{Sp140}$ structure (PDB ID: 6G8R), PHD$_{Sp140}$ residues showing significant CSP (N662, E665, C666, E667, F685, H686, H690, I691, C703, C706) clustered around the Zn^{2+} coordination sites and on the side facing the BRD in the tandem domain context (Fig. 3c). This interaction surface was reminiscent of the one observed for PHD-BRD$_{Kap1/TRIM28}$, where the Zn^{2+} binding residues of the PHD finger and part of its interface with the adjacent BRD domain were mostly affected, implying a structural rearrangement of the tandem domain to accommodate Ubc9 [27,41]. Reversed NMR titrations, performed adding PHD-BRD$_{Sp140}$ (Fig. 4a,b) or PHD$_{Sp140}$ (Fig. 4d,e) into ^{15}N labelled Ubc9, confirmed binding, as assessed by peaks disappearance and CSPs, mainly around the Ubc9 catalytic C97 (Fig. 4c,f).

Finally, line-broadening effects along with small but significant

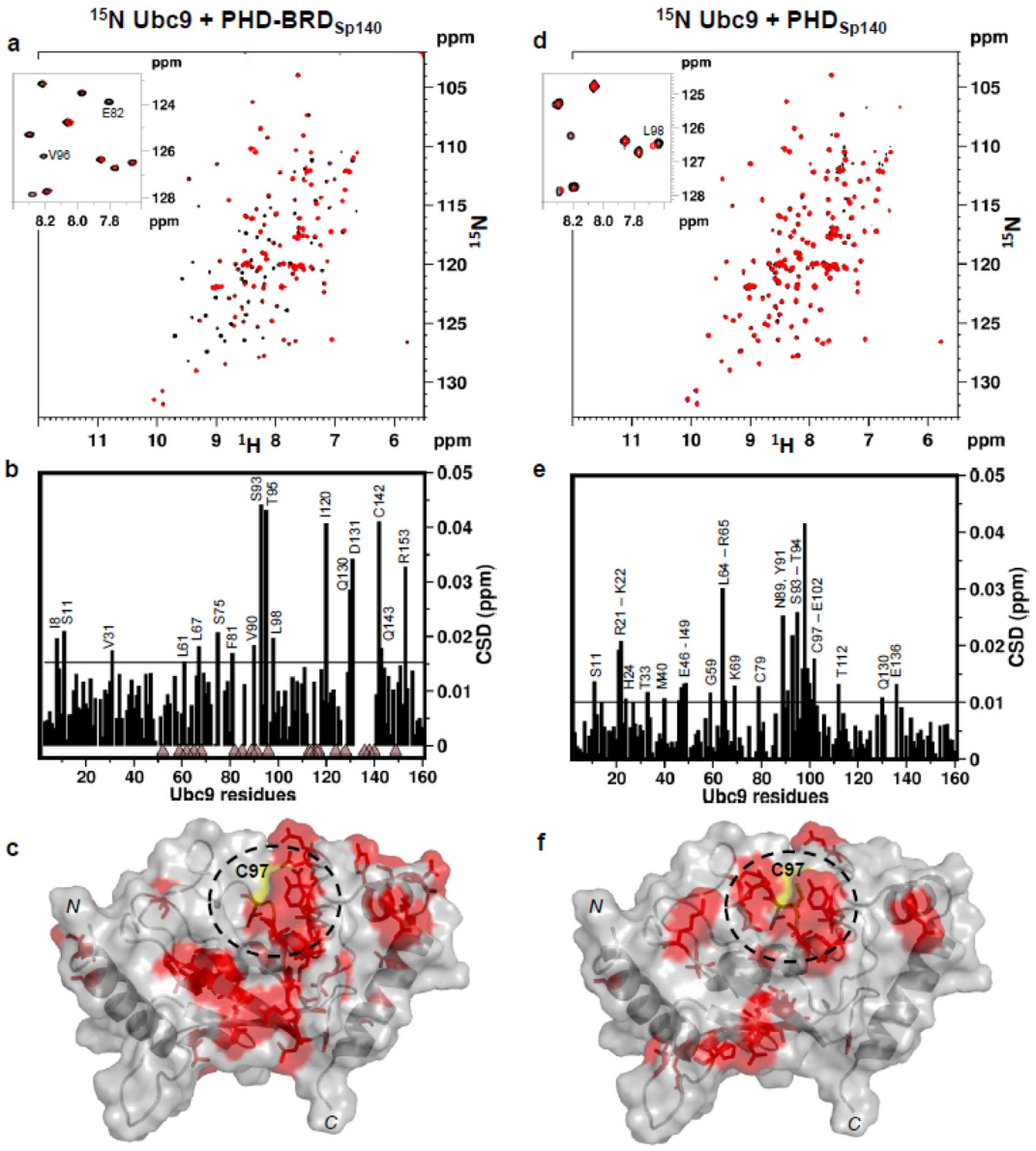

Fig. 4. ^{15}N Ubc9 interacts with PHD-BRD$_{Sp140}$ and PHD$_{Sp140}$.
(a) Overlaid ^{1}H-^{15}N HSQC spectra of 0.1 mM ^{15}N Ubc9 without (black) and with (red) 4-fold excess of PHD-BRD$_{Sp140}$ In the inset is represented a zoomed region of the overlaid spectra, with residues showing peaks displacement/disappearance upon binding. (b) Histograms showing the averaged amide CSPs observed for ^{15}N Ubc9 residues upon PHD-BRD$_{Sp140}$ addition. Missing bars correspond to either prolines or to amides exchanging with the solvent. The triangles indicate peaks disappeared upon binding. Residues with CSP > AVG + σ_{corr} (horizontal line) are labelled. (c) Surface representation of Ubc9 (PDB ID:1A3S), residues showing significant CSP (CSP > AVG + σcorr) upon PHD-BRD$_{Sp140}$ addition are reported in red, the catalytic C97 is reported in yellow and explicitly labelled. (d) Overlaid ^{1}H-^{15}N HSQC spectra of 0.1 mM ^{15}N Ubc9 without (black) and with (red) 4-fold excess of PHD$_{Sp140}$. In the inset is represented a zoomed region of the overlaid spectra, with residues showing peaks displacement/disappearance upon binding. (e) Histograms showing the averaged amide CSPs observed for ^{15}N Ubc9 residues upon PHD$_{Sp140}$ addition. Missing bars correspond to either prolines or to amides exchanging with the solvent. The triangles indicate peaks disappeared upon binding. Residues with CSP > AVG + σ_{corr} (horizontal line) are labelled. (f) Surface representation of Ubc9 (PDB ID:1A3S), residues showing significant CSP (CSP > AVG + σcorr) upon PHD$_{Sp140}$ addition are reported in red, the catalytic C97 is reported in yellow and explicitly labelled.

CSPs observed in NMR titrations of SUMO-1 into ^{15}N PHD-BRD$_{Sp140}$ (Fig. 3d,e) and ^{15}N PHD$_{Sp140}$ (Supporting Information Fig. S7c,d) proved interaction with SUMO-1. PHD$_{Sp140}$ residues significantly affected by SUMO-1 binding (N662, D664, E665, C666, F676, E697, R698, N702, F705, C706, K709) when mapped on the PHD-BRD$_{Sp140}$ (Fig. 3f) partially differed from the one involved in Ubc9 interaction, in line with the ability of PHD fingers to work as structural hubs for multiple interactions [42–45]. Collectively, these results support the notion that the PHD finger and the PHD-BRD$_{Sp140}$ cassette can work as suitable docking platform for the fundamental components of the SUMOylation machinery.

3.5. The PHD finger integrity is required for the SUMOylation of the adjacent BRD domain

To assess the functional importance of the structural integration between PHD and BRD tandem domains, we asked whether the PHD finger within the context of the PHD-BRD$_{Sp140}$ cassette was necessary to promote the SUMOylation of the adjacent BRD domain. Indeed previous *in vitro* SUMOylation experiments performed on PHD-BRD$_{Kap1/Trim28}$ showed that the PHD finger integrity was required to promote intramolecular BRD SUMOylation [41]. To verify this hypothesis, we performed *in vitro* SUMOylation of His$_6$-GST-PHD-BRD$_{Sp140}$ (SP140PB)

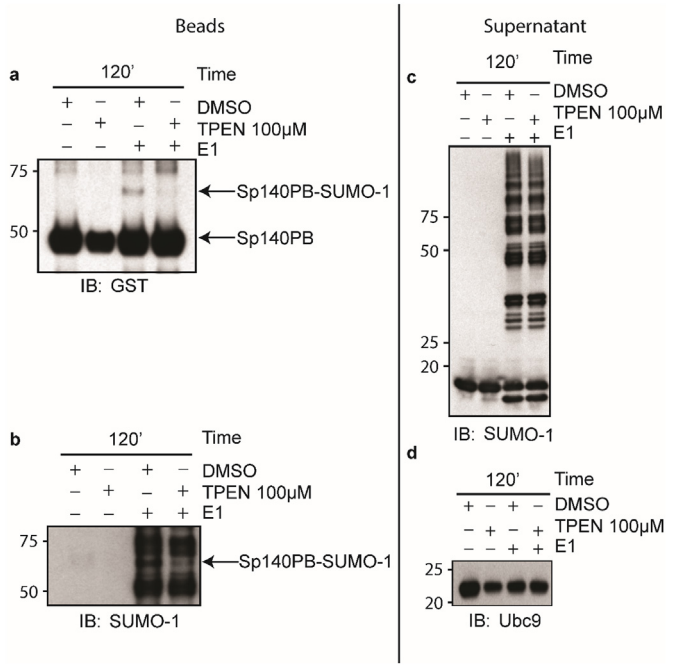

Fig. 5. The integrity of the PHD finger of Sp140 is required for SUMOylation of the adjacent BRD. Immobilized His_6-GST-PHD-BRD_{Sp140} (SP140PB) was incubated with E1, Ubc9 and SUMO-1 for 120 min at 30 °C in the presence of 100 μM TPEN or DMSO as negative control. To reduce the complexity of the sample and evaluate the effects of TPEN on SP140PB SUMOylation, the immobilized protein on the beads (a, b) was analyzed through western blot with the indicated antibodies, separately by the supernatant (c, d), where all the intermediates of the SUMOylation reaction can be detected. Arrows indicate the band corresponding to SP140PB with or without SUMOylation. Reactions without E1 enzyme were used as controls.

after having treated it with 100 μM N,N,N′,N′-tetrakis (2-pyridinylmethyl)-1,2-ethanediamine (TPEN). TPEN is a well-established Zn^{2+}-chelator, commonly used to destabilize PHD fingers or RING fingers working as E3 ligase [46]. Indeed TPEN destabilized the Zn^{2+}-dependent PHD_{Sp140} fold while maintaining the BRD integrity, as shown by CD and NMR spectroscopy (Supporting Information Fig S8a,b,c). As a consequence, PHD finger destabilization by TPEN abrogated its interaction with Ubc9, as indicated by the absence of perturbations in the ^{1}H-^{15}N HSQC spectrum of TPEN-treated ^{15}N PHD_{Sp140} upon Ubc9 addition (Supporting Information Fig. S8d). Accordingly, sample pre-treatment with TPEN abrogated *in vitro* SUMOylation of Sp140PB, as pointed out by the absence of the high molecular weight SUMO-1 conjugate (Fig. 5, Supporting Information Fig. S9a). Of note, TPEN pre-treatment of the well-known positive control substrate GST-RanGAP1 fragment did not affect substrate SUMOylation (Supporting Information Fig. S9b), thus excluding any TPEN interference in E1 or E2 enzymatic activities. Collectively, these data indicate that in the context of the PHD-BRD_{Sp140} cassette the PHD_{Sp140} integrity is required as Ubc9 docking surface for the SUMOylation of the adjacent BRD.

4. Conclusions

As a contribution to Sp140 molecular characterization, we have reported here for the first time, that endogenous Sp140 is a SUMO-1 target. Moreover, using a sophisticated proteomic strategy we have provided the first site-specific molecular evidence that Sp140 is a strong substrate for multiple SUMO-1 conjugation. We identified 13 SUMOylation sites distributed along the entire protein sequence between and within its chromatin binding domains SAND and BRD, suggesting a modulatory effect of Sp140 chromatin recruitment upon SUMOylation. In particular, *in vitro* SUMOylation experiments and NMR titrations performed on PHD-BRD_{Sp140} cassette demonstrated that this tandem domain is an interaction platform suitable for SUMOylation, whereby the PHD finger works as a versatile protein-protein interaction module assisting intramolecular SUMOylation of the adjacent BRD. Interestingly, very recently a direct involvement of PHD fingers in SUMOylation reactions has been also observed in other PHD-BRD containing proteins, such as TRIM24 [24], or the CREB-binding protein catalytic core. In the latter, NMR titrations and *in vitro* SUMOylation assays demonstrated that BRD, PHD, and ZZ domains function in synergism as SUMO E3 ligase to promote intramolecular SUMOylation of the cysteine rich domain CRD1 [47]. Collectively, our results strengthen the concept that combinatorial association of chromatin binding domains, such as PHD and BRD domains, generates a multifaceted interaction scaffold, whose function goes beyond the canonical histone binding activity. SUMOylation is turning out as a general important process in the regulation of immunity [48] and in a broader context, as a many-sided PTM that can cross-talk with other chromatin epigenetic modifications, herewith regulating gene expression [24]. Moreover, multi-SUMOylation is emerging as a new mechanism for the specific recruitment of coregulatory proteins that contain multi-SUMO Interaction motifs (SIMs) [49]. The addition of Sp140 to the increasing lists of multi-SUMOylated proteins opens therefore new perspectives for molecular studies on Sp140 transcriptional activity, where multi-SUMOylation could represent a regulatory route and a docking surface for the recruitment and assembly of leukocyte-specific transcription regulators endowed with multi-SIMs. In conclusion, this work and a previous study, demonstrating PIN1-mediated peptidyl-prolyl isomerization upon threonine phosphorylation of PHD_{Sp140} E3 loop [32], support the notion that Sp140 is regulated by post-translational modifications. More work is needed to further explore how these PTMs orchestrate Sp140 cellular function.

Acknowledgements

AB thanks the Functional Protemic Unit for technical support and discussions. ST thanks Dr. Elena Maspero and Dr. Carlos Nino (IFOM, Milan) for scientific discussion and help with the biochemical part. We thank Prof. Pärt Peterson (University of Tartu, Estonia), Dr. Marc David Ruepp, (University of Bern, Switzerland), for pFLAG-Sp140-CMV-5a plasmids providing and pCDH-His6-SUMO-1T95K, respectively. ST conducted this study as partial fulfillment of his PhD in Molecular Medicine, Program in Cellular and Molecular Biology, San Raffaele University, Milan, Italy. CZ conducted this study as partial fulfillment of her PhD in Biochemistry, University of Milan, Italy.

This work was supported by Italian Association for Cancer Research AIRC [to GM, IG-13159; IG-17468, to AB IG 18607], by Italian Ministry for Health [to GM RF-2013-02354880].

Data references

The mass spectrometry data from this publication have been deposited to the PeptideAtlas database [http://www.peptideatlas.org/PASS/PASS01098] and assigned the identifier PASS01098.

Appendix A. Supplementary data

Supplementary data to this article can be found online at https://doi.org/10.1016/j.bbagen.2018.11.011.

References

[1] S. Mehta, D.A. Cronkite, M. Basavappa, T.L. Saunders, F. Adiliaghdam, H. Amatullah, S.A. Morrison, J.D. Pagan, R.M. Anthony, P. Tonnerre, G.M. Lauer, J.C. Lee, S. Digumarthi, L. Pantano, S.J. Ho Sui, F. Ji, R. Sadreyev, C. Zhou, A.C. Mullen, V. Kumar, Y. Li, C. Wijmenga, R.J. Xavier, T.K. Means, K.L. Jeffrey, Maintenance of macrophage transcriptional programs and intestinal homeostasis by epigenetic reader SP140, Sci. Immunol. 2 (2017) eaag3160, , https://doi.org/10.

1126/sciimmunol.aag3160.
[2] M. Saare, U. Hämarik, R. Venta, M. Panarina, C. Zucchelli, M. Pihlap, A. Remm, K. Kisand, U. Toots, K. Moll, R. Salupere, G. Musco, R. Uibo, P. Peterson, SP140L, an evolutionarily recent member of the sp100 family, is an autoantigen in primary biliary cirrhosis, J Immunol Res (2015) (2015) 526518, https://doi.org/10.1155/2015/526518.
[3] A. Granito, W.H. Yang, L. Muratori, M.J. Lim, A. Nakajima, S. Ferri, G. Pappas, C. Quarneti, F.B. Bianchi, D.B. Bloch, P. Muratori, PML nuclear body component sp140 is a novel autoantigen in primary biliary cirrhosis, Am. J. Gastroenterol. 105 (2010) 125–131, https://doi.org/10.1038/ajg.2009.596.
[4] N. Madani, R. Millette, E.J. Platt, M. Marin, S.L. Kozak, D.B. Bloch, D. Kabat, Implication of the lymphocyte-specific nuclear body protein Sp140 in an innate response to human immunodeficiency virus type 1, J. Virol. 76 (2002) 11133–11138, https://doi.org/10.1128/jvi.76.21.11133-11138.2002.
[5] S. Sawcer, G. Hellenthal, M. Pirinen, C.C.A. Spencer, N.A. Patsopoulos, L. Moutsianas, Z. Su, C. Freeman, S.E. Hunt, S. Edkins, E. Gray, R. David, S.C. Potter, A. Goris, G. Band, A.B. Oturai, A. Strange, M. Comabella, N. Hammond, I. Kockum, O.T. McCann, M. Ban, S. Dronov, N. Robertson, S.J. Bumpstead, F. Lisa, T. International, M. Sclerosis, G. Consortium, W.T. Case, C.C. Wtccc, Genetic risk and a primary role for cell-mediated immune mechanisms in multiple sclerosis, Nature 476 (2012) 214–219, https://doi.org/10.1038/nature10251.Genetic.
[6] F. Matesanz, V. Potenciano, M. Fedetz, P. Ramos-Mozo, M. del Mar Abad-Grau, M. Karaky, C. Barrionuevo, G. Izquierdo, J.L. Ruiz-Peña, M.I. García-Sánchez, M. Lucas, Ó. Fernández, L. Leyva, D. Otaegui, M. Muñoz-Culla, J. Olascoaga, K. Vandenbroeck, I. Alloza, I. Astobiza, A. Antigüedad, L.M. Villar, J.C. Álvarez-Cermeño, S. Malhotra, M. Comabella, X. Montalban, A. Saiz, Y. Blanco, R. Arroyo, J. Varadé, E. Urcelay, A. Alcina, A functional variant that affects exon-skipping and protein expression of SP140 as genetic mechanism predisposing to multiple sclerosis, Hum. Mol. Genet. 24 (2015) 5619–5627, https://doi.org/10.1093/hmg/ddv256.
[7] M. Karaky, M. Fedetz, V. Potenciano, E. Andrés-León, A.E. Codina, C. Barrionuevo, A. Alcina, F. Matesanz, SP140 regulates the expression of immune-related genes associated with multiple sclerosis and other autoimmune diseases by NF-κB inhibition, Hum. Mol. Genet. (2018) 1–43, https://doi.org/10.1093/hmg/ddy284.
[8] A. Franke, D.P.B. McGovern, J.C. Barrett, K. Wang, et al., M. Parkes, Genome-wide meta-analysis increases to 71 the number of confirmed Crohn's disease susceptibility loci, Nat. Genet. 42 (2010) 1118–1125, https://doi.org/10.1038/ng.717.
[9] L. Jostins, S. Ripke, R.K. Weersma, R.H. Duerr, P. Whittaker, et al., Host-microbe interactions have shaped the genetic architecture of inflammatory bowel disease, Nature 491 (2012) 119–124, https://doi.org/10.1038/nature11582.
[10] M.C. Di Bernardo, D. Crowther-Swanepoel, P. Broderick, E. Webb, G. Sellick, R. Wild, K. Sullivan, J. Vijayakrishnan, Y. Wang, A.M. Pittman, N.J. Sunter, A.G. Hall, M.J.S. Dyer, E. Matutes, C. Dearden, T. Mainou-Fowler, G.H. Jackson, G. Summerfield, R.J. Harris, A.R. Pettitt, P. Hillmen, D.J. Allsup, J.R. Bailey, G. Pratt, C. Pepper, C. Fegan, J.M. Allan, D. Catovsky, R.S. Houlston, A genome-wide association study identifies six susceptibility loci for chronic lymphocytic leukemia, Nat. Genet. 40 (2008) 1204–1210, https://doi.org/10.1038/ng.219.
[11] Q. Lan, W.-Y. Au, S. Chanock, J. Tse, K. Wong, M. Shen, L.P. Siu, J. Yuenger, M. Yeager, H.D. Hosgood III, M.P. Purdue, R. Liang, N. Rothman, Genetic susceptibility for chronic lymphocytic leukemia among Chinese in Hong Kong, Eur. J. Haematol. 85 (2010) 492–495, https://doi.org/10.1111/j.1600-0609.2010.01518.x.
[12] F.C.M. Sillé, R. Thomas, M.T. Smith, L. Conde, C.F. Skibola, Post-GWAS functional characterization of susceptibility variants for chronic lymphocytic leukemia, PLoS ONE 7 (2012) e29632, , https://doi.org/10.1371/journal.pone.0029632.
[13] V. Quesada, L. Conde, N. Villamor, G.R.e.al. Ordóñez, C. López-Otín, Exome sequencing identifies recurrent mutations of the splicing factor SF3B1 gene in chronic lymphocytic leukemia, Nat. Genet. 44 (2012) 47–52, https://doi.org/10.1038/ng.1032.
[14] N. Bolli, H. Avet-Loiseau, D.C. Wedge, P. Van Loo, L.B. Alexandrov, I. Martincorena, K.J. Dawson, F. Iorio, S. Nik-Zainal, P.J. Campbell, N.C. Munshi, et al., Heterogeneity of genomic evolution and mutational profiles in multiple myeloma, Nat. Commun. 5 (2014) 1–13, https://doi.org/10.1038/ncomms3997.
[15] D.B. Bloch, A. Nakajima, T. Gulick, J.D. Chiche, D. Orth, S.M. de La Monte, K.D. Bloch, Sp110 localizes to the PML-Sp100 nuclear body and may function as a nuclear hormone receptor transcriptional coactivator, Mol. Cell. Biol. 20 (2000) 6138–6146, https://doi.org/10.1128/MCB.20.16.6138-6146.2000.
[16] J.S. Seeler, A. Marchio, R. Losson, J.M. Desterro, R.T. Hay, P. Chambon, A. Dejean, Common properties of nuclear body protein SP100 and TIF1alpha chromatin factor: role of SUMO modification, Mol. Cell. Biol. 21 (2001) 3314–3324, https://doi.org/10.1128/MCB.21.10.3314-3324.2001.
[17] M.J. Bottomley, M.W. Collard, J.I. Huggenvik, Z. Liu, T.J. Gibson, M. Sattler, The SAND domain structure defines a novel DNA-binding fold in transcriptional regulation, Nat. Struct. Biol. 8 (2001) 626–633, https://doi.org/10.1038/89675.
[18] C.A. Musselman, M.E. Lalonde, J. Côté, T.G. Kutateladze, Perceiving the epigenetic landscape through histone readers, Nat. Struct. Mol. Biol. 19 (2012) 1218–1227, https://doi.org/10.1038/nsmb.2436.
[19] R. Sanchez, J. Meslamani, M. Zhou, The bromodomain: from epigenome reader to druggable target, BBA - Gene Regul. Mech. 1839 (2014) 676–685, https://doi.org/10.1016/j.bbagrm.2014.03.011.
[20] P. Filippakopoulos, S. Picaud, M. Mangos, T. Keates, J.P. Lambert, D. Barsyte-Lovejoy, I. Felletar, R. Volkmer, S. Müller, T. Pawson, A.C. Gingras, C.H. Arrowsmith, S. Knapp, Histone recognition and large-scale structural analysis of the human bromodomain family, Cell 149 (2012) 214–231, https://doi.org/10.1016/j.cell.2012.02.013.
[21] R. Sanchez, M.-M. Zhou, The role of human bromodomains in chromatin biology and gene transcription, Curr. Opin. Drug Discov. Devel. 12 (2009) 659–665, https://doi.org/10.1016/j.bbi.2008.05.010.
[22] M.M. Zhou, Histone Recognition, Histone Recognit, (2015), pp. 1–282, https://doi.org/10.1007/978-3-319-18102-8.
[23] W.W. Tsai, Z. Wang, T.T. Yiu, K.C. Akdemir, W. Xia, S. Winter, C.Y. Tsai, X. Shi, D. Schwarzer, W. Plunkett, B. Aronow, O. Gozani, W. Fischle, M.C. Hung, D.J. Patel, M.C. Barton, TRIM24 links a non-canonical histone signature to breast cancer, Nature 468 (2010) 927–932, https://doi.org/10.1038/nature09542.
[24] S. Appikonda, K.N. Thakkar, P.K. Shah, S.Y.R. Dent, J.N. Andersen, M.C. Barton, Cross-talk between chromatin acetylation and SUMOylation of tripartite motif–containing protein 24 (TRIM24) impacts cell adhesion, J. Biol. Chem. 293 (2018) 7486–7487, https://doi.org/10.1074/jbc.RA118.002233.
[25] Q. Xi, Z. Wang, A.I. Zaromytidou, X.H.F. Zhang, L.F. Chow-Tsang, J.X. Liu, H. Kim, A. Barlas, K. Manova-Todorova, V. Kaartinen, L. Studer, W. Mark, D.J. Patel, J. Massagué, A poised chromatin platform for TGF-β access to master regulators, Cell 147 (2011) 1511–1524, https://doi.org/10.1016/j.cell.2011.11.032.
[26] X. Zhang, D. Zhao, X. Xiong, Z. He, H. Li, Multifaceted histone H3 methylation and phosphorylation readout by the plant homeodomain finger of human nuclear antigen Sp100C, J. Biol. Chem. 291 (2016) 12786–12798, https://doi.org/10.1074/jbc.M116.721159.
[27] L. Zeng, K.L. Yap, A.V. Ivanov, X. Wang, S. Mujtaba, O. Plotnikova, F.J. Rauscher, M.M. Zhou, Structural insights into human KAP1 PHD finger-bromodomain and its role in gene silencing, Nat. Struct. Mol. Biol. 15 (2008) 626–633, https://doi.org/10.1038/nsmb.1416.
[28] K. Eifler, A.C.O. Vertegaal, SUMOylation-mediated regulation of cell cycle progression and cancer, Trends Biochem. Sci. 40 (2015) 779–793, https://doi.org/10.1016/j.tibs.2015.09.006.
[29] S.P. Jackson, D. Durocher, Regulation of DNA damage responses by Ubiquitin and SUMO, Mol. Cell 49 (2013) 795–807, https://doi.org/10.1016/j.molcel.2013.01.017.
[30] F. Melchior, M. Schergaut, A. Pichler, SUMO: ligases, isopeptidases and nuclear pores, Trends Biochem. Sci. 28 (2003) 612–618, https://doi.org/10.1016/j.tibs.2003.09.002.
[31] T. Sternsdorf, K. Jensen, B. Reich, H. Will, The nuclear dot protein Sp100, characterization of domains necessary for dimerization, subcellular localization, and modification by small ubiquitin- like modifiers, J. Biol. Chem. 274 (1999) 12555–12566, https://doi.org/10.1074/jbc.274.18.12555.
[32] C. Zucchelli, S. Tamburri, G. Quilici, E. Palagano, A. Berardi, M. Saare, P. Peterson, A. Bachi, G. Musco, Structure of human Sp140 PHD finger: an atypical fold interacting with Pin1, FEBS J. 281 (2014) 216–231, https://doi.org/10.1111/febs.12588.
[33] A. Pichler, A. Gast, J.S. Seeler, A. Dejean, F. Melchior, The nucleoporin RanBP2 has SUMO1 E3 ligase activity, Cell 108 (2002) 109–120, https://doi.org/10.1016/S0092-8674(01)00633-X.
[34] J. Schleucher, M. Schwendinger, M. Sattler, P. Schmidt, O. Schedletzky, S.J. Glaser, O.W. Sørensen, C. Griesinger, A general enhancement scheme in heteronuclear multidimensional NMR employing pulsed field gradients, J. Biomol. NMR 4 (1994) 301–306, https://doi.org/10.1007/BF00175254.
[35] C. Griesinger, M. Sattler, Heteronuclear Multidimensional NMR Experiments for the Structure Determination of Proteins in Solution Employing Pulsed Field Gradients, Vol. 34 (1999), pp. 93–158.
[36] S. Grzesiek, S.J. Stahl, P.T. Wingfield, A. Bax, The CD4 determinant for downregulation by HIV-1 Nef directly binds to Nef. Mapping of the Nef binding surface by NMR, Biochemistry 35 (1996) 10256–10261, https://doi.org/10.1021/bi9611164.
[37] F.H. Schumann, Æ.H. Riepl, Æ.T. Maurer, Æ.W. Gronwald, K.N.Æ. Hans, R. Kalbitzer, Combined Chemical Shift Changes and Amino Acid Specific Chemical Shift Mapping of Protein – Protein Interactions, (2007), pp. 275–289, https://doi.org/10.1007/s10858-007-9197-z.
[38] N. Guex, M.C. Peitsch, T. Schwede, Automated comparatice protein structure modelling with SWISS-MODEL and Swiss-Pdb Viewer: a historical perspective, Electrophoresis 30 (2009) S162–S173, https://doi.org/10.1002/elps.200900140.
[39] I. Sengupta, D. Das, S.P. Singh, R. Chakravarty, C. Das, Host transcription factor Speckled 110kDa (Sp110), a nuclear body protein, is hijacked by Hepatitis B virus protein X for viral persistence, J. Biol. Chem. 292 (2017), https://doi.org/10.1074/jbc.M117.796839 jbc.M117.796839.
[40] T. Tammsalu, I. Matic, E.G. Jaffray, A.F.M. Ibrahim, M.H. Tatham, R.T. Hay, Proteome-wide identification of SUMO2 modification sites, Sci. Signal. 7 (2014) rs2, https://doi.org/10.1126/scisignal.2005146.
[41] A.V. Ivanov, H. Peng, V. Yurchenko, K.L. Yap, D.G. Negorev, D.C. Schultz, E. Psulkowski, W.J. Fredericks, D.E. White, G.G. Maul, M.J. Sadofsky, M.M. Zhou, F.J. Rauscher, PHD domain-mediated E3 ligase activity directs intramolecular sumoylation of an adjacent bromodomain required for gene silencing, Mol. Cell 28 (2007) 823–837, https://doi.org/10.1016/j.molcel.2007.11.012.
[42] C.A. Musselman, T.G. Kutateladze, Handpicking epigenetic marks with PHD fingers, Nucleic Acids Res. 39 (2011) 9061–9071, https://doi.org/10.1093/nar/gkr613.
[43] S. Park, R.L. Stanfield, M.A. Martinez-Yamout, H.J. Dyson, I.A. Wilson, Role of the CBP Catalytic Core in Intramolecular SUMOylation and Control of Histone H3 Acetylation, (2017), https://doi.org/10.1073/pnas.1703105114.
[44] M. Fiedler, M.J. Sanchez-Barrena, M. Nekrasov, J. Mieszczanek, V. Rybin, J. Mueller, P. Evans, M. Bienz, Decoding of methylated histone H3 tail by the Pygo-BCL9 Wnt signaling complex, Mol. Cell 30 (2008) 507–518, https://doi.org/10.1016/j.molcel.2008.03.011.
[45] M. Gaetani, V. Matafora, M. Saare, D. Spiliotopoulos, L. Mollica, G. Quilici, F. Chignola, Valeria Mannella, C. Zucchelli, P. Peterson, A. Bachi, G. Musco, AIRE-PHD fingers are structural hubs to maintain the integrity of chromatin-associated

interactome, Nucleic Acids Res. 40 (2012) 11756–11768, https://doi.org/10.1093/nar/gks933.
[46] B.E. Dul, N.C. Walworth, The plant homeodomain fingers of fission yeast Msc1 exhibit E3 ubiquitin ligase activity, J. Biol. Chem. 282 (2007) 18397–18406, https://doi.org/10.1074/jbc.M700729200.
[47] S. Park, R.L. Stanfield, M.A. Martinez-Yamout, H.J. Dyson, I.A. Wilson, P.E. Wright, Role of the CBP catalytic core in intramolecular SUMOylation and control of histone H3 acetylation, Proc. Natl. Acad. Sci. 114 (2017) E5335–E5342, https://doi.org/10.1073/pnas.1703105114.
[48] Z. Hannoun, G. Maarifi, M.K. Chelbi-Alix, The implication of SUMO in intrinsic and innate immunity, Cytokine Growth Factor Rev. 29 (2016) 3–16, https://doi.org/10.1016/j.cytogfr.2016.04.003.
[49] E. Aguilar-Martinez, X. Chen, A. Webber, A.P. Mould, A. Seifert, R.T. Hay, A.D. Sharrocks, Screen for multi-SUMO–binding proteins reveals a multi-SIM–binding mechanism for recruitment of the transcriptional regulator ZMYM2 to chromatin, Proc. Natl. Acad. Sci. 112 (2015) E4854–E4863, https://doi.org/10.1073/pnas.1509716112.